ADVANCES IN ATMOSPHERIC SCIENCES, VOL. 35, AUGUST 2018, 955–964

• **Original Paper** •

Skillful Seasonal Forecasts of Summer Surface Air Temperature in Western China by Global Seasonal Forecast System Version 5

Chaofan LI*[1], Riyu LU[2,3], Philip E. BETT[4], Adam A. SCAIFE[4,5], and Nicola MARTIN[4]

[1]*Center for Monsoon System Research, Institute of Atmospheric Physics, Chinese Academy of Sciences, Beijing* 100029*, China*

[2]*State Key Laboratory of Numerical Modelling for Atmospheric Sciences and Geophysical Fluid Dynamics, Institute of Atmospheric Physics, Chinese Academy of Sciences, Beijing* 100029*, China*

[3]*University of the Chinese Academy of Sciences, Beijing* 100029*, China*

[4]*Met Office Hadley Centre, FitzRoy Road, Exeter* EX1 3PB*, UK*

[5]*College of Engineering, Mathematics and Physical Sciences, University of Exeter, Exeter, Devon* EX4 4QF*, UK*

(Received 16 November 2017; revised 3 March 2018; accepted 3 April 2018)

ABSTRACT

Variations of surface air temperature (SAT) are key in affecting the hydrological cycle, ecosystems and agriculture in western China in summer. This study assesses the seasonal forecast skill and reliability of SAT in western China, using the GloSea5 operational forecast system from the UK Met Office. Useful predictions are demonstrated, with considerable skill over most regions of western China. The temporal correlation coefficients of SAT between model predictions and observations are larger than 0.6, in both northwestern China and the Tibetan Plateau. There are two important sources of skill for these predictions in western China: interannual variation of SST in the western Pacific and the SST trend in the tropical Pacific. The tropical SST change in the recent two decades, with a warming in the western Pacific and cooling in the eastern Pacific, which is reproduced well by the forecast system, provides a large contribution to the skill of SAT in northwestern China. Additionally, the interannual variation of SST in the western Pacific gives rise to the reliable prediction of SAT around the Tibetan Plateau. It modulates convection around the Maritime Continent and further modulates the variation of SAT on the Tibetan Plateau via the surrounding circulation. This process is evident irrespective of detrending both in observations and the model predictions, and acts as a source of skill in predictions for the Tibetan Plateau. The predictability and reliability demonstrated in this study is potentially useful for climate services providing early warning of extreme climate events and could imply useful economic benefits.

Key words: seasonal forecast, western China, surface air temperature, predictability, warming trend

Citation: Li, C. F., R. Y. Lu, P. E. Bett, A. A. Scaife, and N. Martin, 2018: Skillful seasonal forecasts of summer surface air temperature in western China by Global Seasonal Forecast System version 5. *Adv. Atmos. Sci.*, **35**(8), 955–964, https://doi.org/10.1007/s00376-018-7291-7.

1. Introduction

Surface air temperature (SAT) is a very important hydrological and climatic variable in western China. In contrast to the monsoon regions in eastern China, most regions in western China are arid, semi-arid or subject to snow cover. Variations of the SAT in western China are thus recognized as key in connecting with heat waves, water resources, agriculture and ecosystems (Qin et al., 2006; Chen et al., 2009; Wei and Chen, 2009). For example, the arid Turpan Basin in northwestern China, produces fruit and cotton but suffers from excessive heat and shortage of water resources, relying heavily on seasonal changes of SAT and the resulting water from snowmelt. Thus, a skillful prediction of summer SAT in western China is in great demand.

Variation of SAT over western China is directly modulated by local ascent rates caused by surrounding anomalous circulations (Qian et al., 2004; Chen et al., 2009). A warm SAT anomaly tends to occur in association with anomalous descending air motion, increased low-level geopotential height and anticyclonic circulation, and vice versa. Factors that relate to changes in these circulation anomalies, like tropical air–sea interactions (Ding and Wang, 2005; Huang et al., 2011), potentially imply a remote teleconnection with the variation of SAT over western China, but are not yet well demonstrated. In addition, variation of SAT over western China is quite sensitive to climate change, and shows remarkable warming since the 1980s (Zhou and Huang, 2003, 2010). As a result, this variation links with a strong increase

* Corresponding author: Chaofan LI
Email: lichaofan@mail.iap.ac.cn

of extreme heat days in northwestern China during the last 40 years (Wei and Chen, 2009).

Along with recent advances in climate models and long-range forecasting, skillful seasonal predictions for some variables have been possible (e.g., Wang, 2008; Li et al., 2012; Scaife et al., 2014) and are becoming more useful in economic planning and disaster mitigation (Ma et al., 2015; Svensson et al., 2015; Palin et al., 2016; Clark et al., 2017; Li et al., 2017). Nevertheless, seasonal forecast skill and reliability of SAT in western China have until recently been elusive. Recently, Bett et al. (2017) assessed the overall seasonal forecast skill of the climate variables relevant to the energy sector in China and showed possible skillful summer prediction of SAT in western China. However, they did not analyze quantitatively the prediction skill of SAT in western China, nor identify the sources of predictability. Further investigations of this predictability and its sources are presented here.

We use the latest Met Office seasonal forecast system—namely, Global Seasonal Forecast System version 5 (GloSea5) (MacLachlan et al., 2015)—to present estimates of summer prediction of the SAT in western China. GloSea5 is a high-resolution, fully coupled atmosphere–ocean forecast system, with initialized stratosphere and sea ice. It has demonstrated considerable capability in predicting the North Atlantic Oscillation (Scaife et al., 2014), Yangtze River valley summer rainfall (Li et al., 2016), winter precipitation over southeastern China (Lu et al., 2017), tropical storms (Camp et al., 2015), as well as wind speed and temperature in the UK and Europe (Clark et al., 2017). As an operational forecast system, GloSea5 has already been effectively applied in China in-real time seasonal forecasts of monsoon rainfall for the Yangtze River Basin (Li et al., 2016; Bett et al., 2018). A better identification in GloSea5 of the summer prediction for SAT in western China will potentially deliver further climate services for this region.

Two main questions will be answered in this study: How well do current coupled models perform in predicting the SAT in western China? And what are the main sources of skill? We first describe the data and hindcast experiments in section 2, then assess the prediction skill and identify the prediction sources in sections 3 and 4, considering the warming trend and interannual variation of the SAT. We finally present our conclusions and discussions in section 5.

2. Data and hindcast experiments

The GloSea5 forecast system is developed based on the second global coupled configuration of HadGEM3 (Williams et al., 2015). The atmospheric resolution is N216 (0.83° in latitude and 0.55° in longitude) and L85 (85 vertical levels reaching to 85 km height). It is coupled with the JULES land surface model (Best et al., 2011), the CICE sea ice model (Rae et al., 2015) and the NEMO ocean model (Megann et al., 2014). The ocean resolution is 0.25° in both latitude and longitude, with 75 levels. More details of the GloSea5 forecast system are given in MacLachlan et al. (2015). We use a set of hindcasts produced by GloSea5 covering 1992 to 2011 for each summer (JJA: June–July–August). There are 24 ensemble members in total, with eight members initialized on each of 25 April, 1 May and 9 May. We use the ensemble mean of these hindcasts in this study.

To verify the model prediction, we use the summer SAT and geopotential height from the ERA-Interim reanalysis (Dee et al., 2011) from 1992 to 2011 as observations. For the summer variation of SAT, we have compared the reanalysis results with an observed 160-station temperature dataset from the China Meteorological Administration, and found that ERA-Interim follows the station data quite well (not shown), as found in previous studies (e.g., Inoue and Matsumoto, 2004; Wu et al., 2005). As the stations are relatively sparse in western China, the spatially complete ERA-Interim reanalysis data are thus a good substitute. Two other datasets, including the monthly precipitation data obtained from GPCP (Adler et al., 2003) and SST data from ERSST.v4 (Huang et al., 2015), were also used for observational verification.

3. Prediction skill of the SAT in western China

We firstly assess the capability of GloSea5 to describe the summer SAT in western China. Figure 1 shows the climatology and interannual variability of JJA-mean SAT in observations and GloSea5. In observations, in addition to the monsoon region in the east, northwestern China suffers from quite hot summers, with the mean temperature exceeding 28°C around the Taklimakan Desert. These high temperatures in northwestern China are the result of dry air adiabatic warming from subsidence associated with surrounding large-scale circulations (Gamo, 1996; Wu and Liu, 2003; Qian et al., 2004). Further south, the mean temperature on the Tibetan Plateau is low because of the high altitude. Temperatures in northern and western China exhibit large interannual variability (Fig. 1c), including both northwestern China and around the Tibetan Plateau, implying an important role for SAT variability in the summer climate. Considering the model predictions, we find that the summer mean and interannual variability are generally well reproduced in GloSea5 (Fig. 1b and 1d).

Figure 2 displays the spatial distribution of prediction skill for SAT in China. The skill score used here is the temporal correlation coefficient between the ensemble mean model prediction and observation at each grid point. It is clear that skillful predictions of SAT are demonstrated by GloSea5 in western China. The prediction skill is significant over most areas of western China and exceeds 0.6 for large areas. This distribution agrees well with Bett et al. (2017), who assessed the skill of temperature for energy demand forecasts, considering the potential for future climate service development. Furthermore, this skill pattern is similar to the longer lead-time prediction correlation of DePreSys3 [version 3 of the UK Met Office Decadal Prediction System; Figs. 1a and c in Monerie et al. (2017)]. This uses the same coupled model as GloSea5 and has a longer hindcast time period from 1960

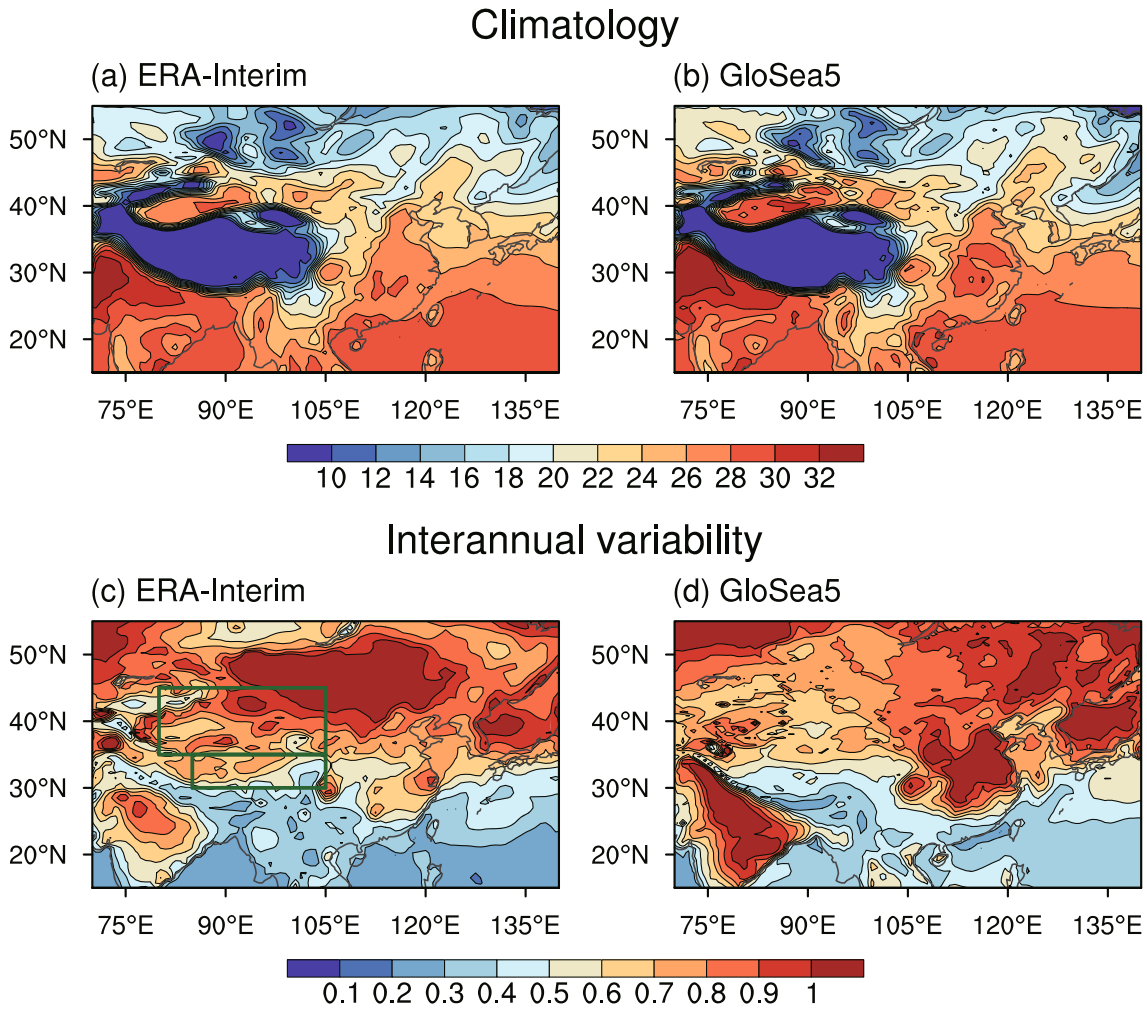

Fig. 1. The (a, b) climatology and (c, d) interannual variability of summer (JJA) mean near-surface air temperature (units: °C) for (a, c) ERA-Interim, as observation, and (b, d) the prediction from GloSea5, from 1992 to 2011. The interannual variability in (d) is characterized by the interannual standard deviation, calculated from all ensemble members and all years. The green boxes indicate the domains of northwestern China (35°–45°N, 80°–105°E) and the Tibetan Plateau (30°–35°N, 85°–105°E).

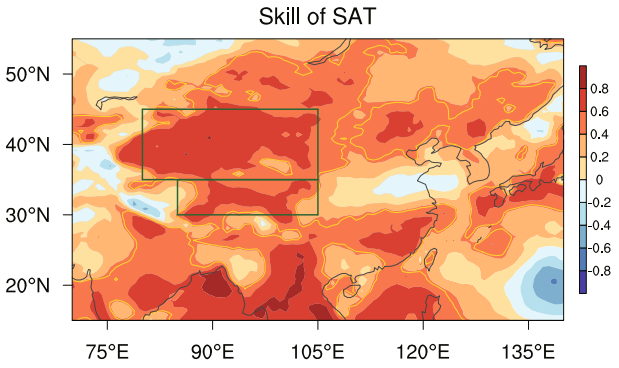

Fig. 2. Prediction skill (temporal correlation coefficient) of summer SAT for the GloSea5 hindcasts. The yellow contours represent gridpoint statistical significance exceeding the 5% significance level. The green boxes indicate the domains of northwestern China (35°–45°N, 80°–105°E) and the Tibetan Plateau (30°–35°N, 85°–105°E).

to 2014. This suggests that the skill of forecasts of SAT in western China achieved by GloSea5 is robust.

To achieve a better understanding of the predictability, we divide western China into two regions, including northwestern China (35°–45°N, 80°–105°E) and the Tibetan Plateau (30°–35°N, 85°–105°E), and define their temperature indices as the area-averaged SAT over these two regions. The reason for us to choose these two regions is their variations of SAT are relatively independent of each other. The correlation coefficient between the two regions is 0.58 (0.42 after detrending) from 1992 to 2011 in observations. Although 0.58 is significant at the 95% confidence level, it still implies that most of the variance is independent between the two regions. Moreover, we have also examined the first two EOFs of SAT in western China. These patterns exhibit anomalies mainly over northwestern China and the Tibetan Plateau, respectively (not shown), further supporting the separate investigation of their sources of skill.

Figure 3 shows the year to year variation of the average summer SAT in northwestern China and the Tibetan Plateau for observations and the predictions. The temperature anomalies are successfully reproduced in most of the years from 1992 to 2011. The correlation coefficients of SAT between the model prediction and observation in northwestern China and the Tibetan Plateau are 0.76 and 0.64, respectively. These are both significant at the 1% significance level according to the Student's *t*-test. These values correspond well to the spatial distribution of prediction skill (Fig. 2) and suggest useful predictions with potentially useful skill levels in the current operational forecast system. In addition, the signal-to-noise ratio, which is defined as the ensemble mean standard deviation divided by the standard deviation of individual members (e.g. Kumar, 2009), is 0.64 for the temperature in these two regions. This is similar to the correlation scores, as it should be for a well calibrated system (Kumar, 2009; Eade et al., 2014) and there is no discrepancy in signal-to-noise ratio in these predictions. Furthermore, systematic warming during the hindcast period is found in these two regions and is well reproduced by the model predictions. The SAT in northwestern China (the Tibetan Plateau) has been increasing at a rate of 0.83°C (0.37°C) per decade in observations, and is reproduced as 0.49°C ±0.17°C (0. 41°C ±0.16°C) per decade in GloSea5. The warming trend is suggested to be an important contributor to the prediction skill of SAT in western China, and will be discussed in the following section.

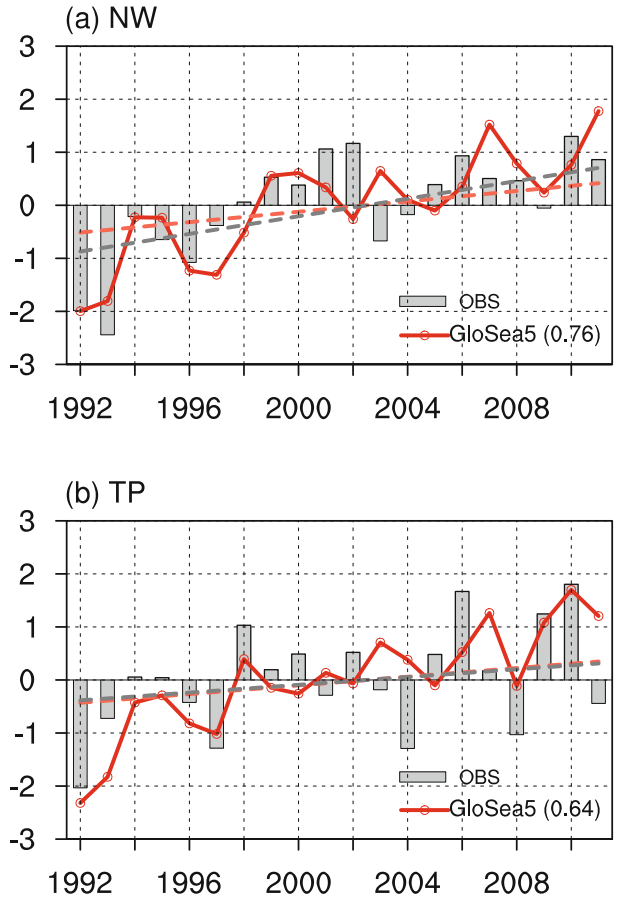

Fig. 3. Normalized time series of SAT in (a) northwestern China and (b) the Tibetan Plateau from observation (bars) and the prediction of GloSea5 (red solid line). The correlation coefficient between the prediction and observation is 0.76 (0.64) over northwestern China (the Tibetan Plateau). Dashed lines represent the linear warming trends.

4. Sources of the prediction skill

4.1. *Warming trend*

Systematic warming associated with skillful prediction is detected in the temperature of western China (Fig. 3). But to what extent does this warming trend contribute to the prediction skill of SAT in western China? Figure 4 shows the spatial distribution of prediction skill for SAT after removing the linear trend. The prediction skill decreases over most regions of China (c.f. Fig. 2). In northwestern China, the correlation coefficient of SAT between the model output and observation declines to 0.45, compared to 0.76 with the trend included (Fig. 3a). It suggests a contribution of the warming trend to the skill of seasonal prediction in this region. Nevertheless, the skill is still generally positive (0.45 just exceeds the 95% confidence level) and is highly significant (> 95%) in South Xinjiang, which is an extremely arid desert area in northwestern China.

The skill around the Tibetan Plateau also remains significant after removing the linear trend. The correlation coefficient of SAT in the Tibetan Plateau between the model prediction and observation is 0.58, similar to the non-detrended result (0.64; Fig. 3b). This implies that the warming trend does not play an important role in the prediction skill of SAT around the Tibetan Plateau, in contrast to the situation in northwestern China. Instead, interannual variations of other factors potentially dominate, and this will be discussed later.

Changes of the prediction skill after detrending are well reflected by the spatial distribution of the linear trend of SAT in China (Fig. 5a). Apparent warming of SAT is found over northwestern China in observations, especially in the northeast with an increase of more than 0.1°C yr^{-1} (corresponding to the regions with large changes of prediction skill when detrending). The regions with strong warming are consistent with those that have a large decrease of prediction skill (Fig. 5b), implying an important role of the warming trend

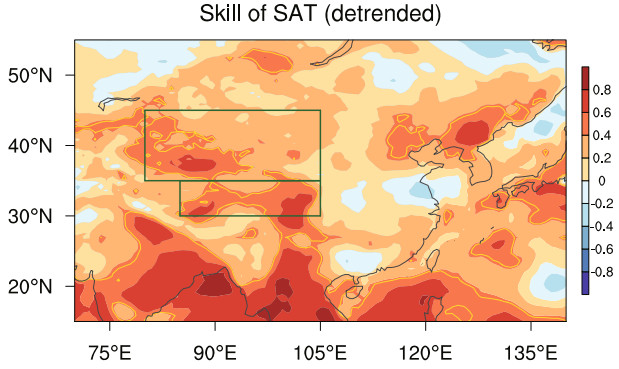

Fig. 4. As in Fig. 2 but for the prediction skill of detrended SAT.

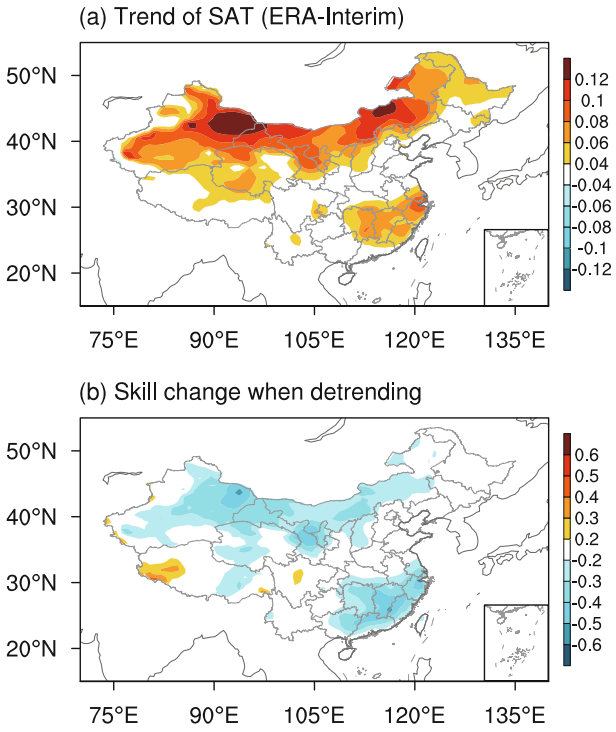

Fig. 5. Spatial distribution for (a) the linear trend of SAT in °C/year and (b) the change of prediction skill when detrending (difference between Figs. 2 and 4).

in the prediction skill of SAT in these regions. This also applies to the summer prediction of SAT in Inner Mongolia and the middle–lower reaches of the Yangtze River Valley, where there is significant skill (Fig. 2) and a large warming trend (Fig. 5).

The tropical SST has a longer memory than the atmosphere and this imparts predictable signals to the tropical atmosphere on seasonal time scales (Wang et al., 2009; Kumar et al., 2013; Scaife et al., 2017); therefore, we search for teleconnections between the SAT in northwestern China and the variations of tropical SST. Figure 6 shows the regressed SST anomalies onto the original and detrended SAT in northwestern China. In association with warm conditions in northwestern China, significant positive SST anomalies in the western Pacific are found in the tropics. These SST anomalies disappear when the warming trend is removed, implying an important role of the warming trend in modulating the teleconnection of SAT in northwestern China to the SST in the tropical Pacific. To identify the sources of predictability, the ensemble mean of all members, which contains more predictable signals, is used as the model prediction. For the SST anomalies in model predictions, the effect of the warming trend can be reasonably reproduced, and shows east–west dipole SST anomalies in the tropical Pacific with or without detrending.

The linear trend in SST during the hindcast period from 1992 to 2011 displays a warming of the tropical western Pacific and cooling of the tropical eastern Pacific that is well captured by the forecast system (Fig. 7). This pattern closely resembles the SST teleconnection pattern associated with high SAT in northwestern China (Fig. 6a) and may therefore explain some of the rapid warming in northwestern China. It further implies the importance of reasonable ocean data assimilation for skillful prediction of SAT in northwestern China, especially in the tropical Pacific Ocean. On seasonal timescales there is very high skill in tropical SST (Wang et al., 2009; Yan et al., 2010; Li et al., 2012) and the ENSO-like pattern shown here. The cooling of the eastern Pacific over this period is likely related to the negative Pacific Decadal Oscillation present in the early 21st century (Ding et al., 2013; Kosaka and Xie, 2016; Smith et al., 2016).

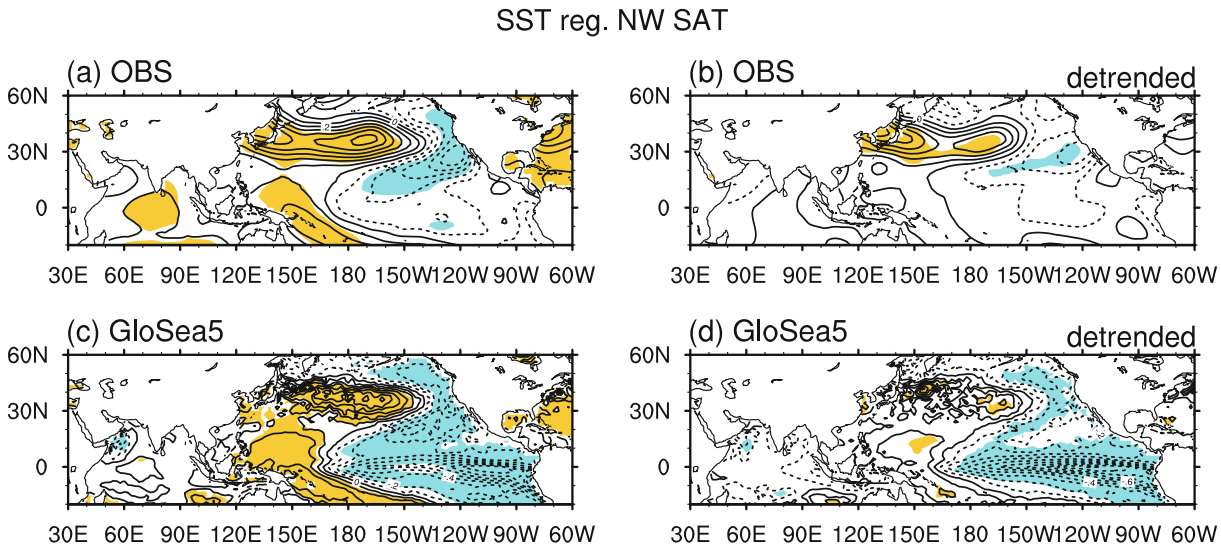

Fig. 6. Regression of SST anomalies onto the (a, c) original and (b, d) detrended SAT in northwestern China for (a, b) observations and (c, d) seasonal predictions. Shading indicates regions where anomalies exceed the 5% significance level. The contour interval is 0.1°C and a positive (negative) anomaly is represented by a solid (dashed) contour.

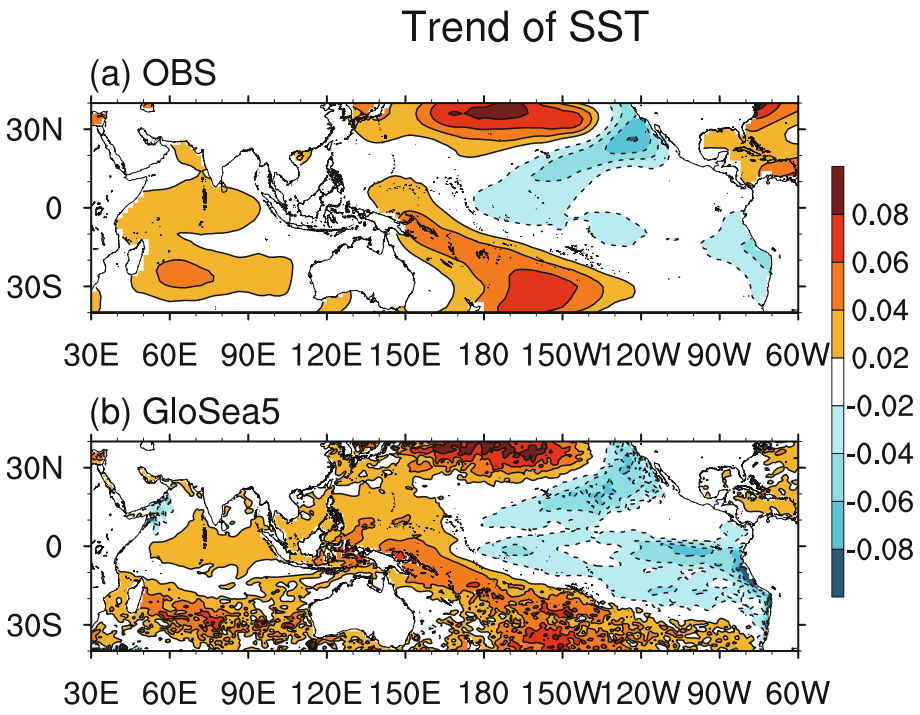

Fig. 7. Spatial distribution for the linear trend of SST (units: °C yr^{-1}) from (a) observations and (b) GloSea5.

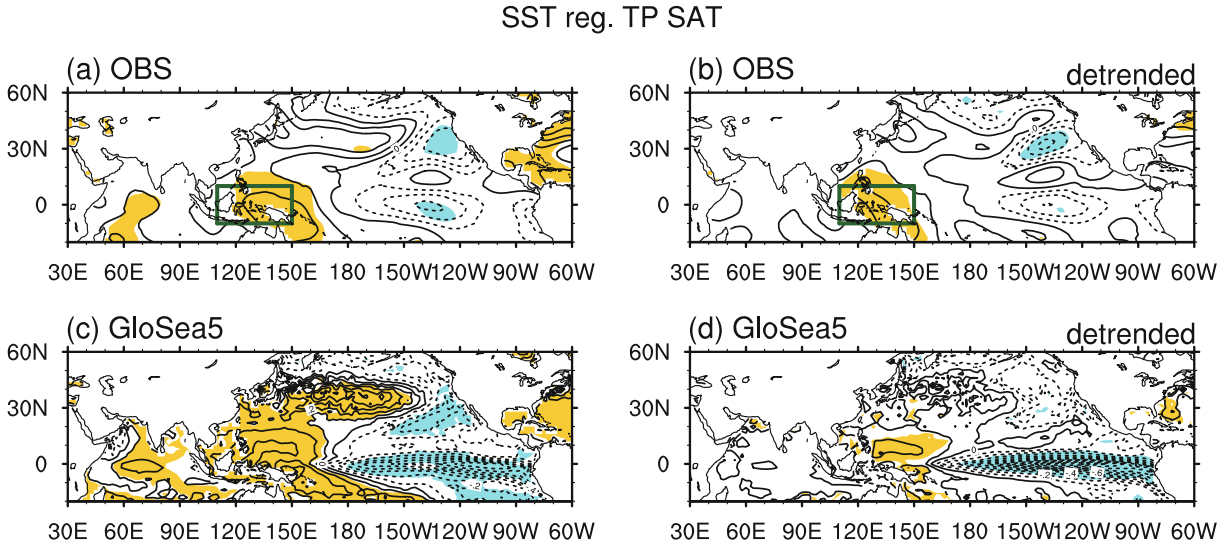

Fig. 8. As in Fig. 6 but for the SAT in the Tibetan Plateau. The green box indicates the key domain of SST anomalies in the western Pacific (10°S–10°N, 110°–150°E).

4.2. *Interannual variation of SST in the western Pacific*

As described earlier, the prediction skill of SAT in the Tibetan Plateau remains high even after removing the linear trend, suggesting that this prediction skill arises mainly from its interannual component. Figure 8 shows the regression of simultaneous SST anomalies onto the SAT in the Tibetan Plateau. Significant warm SST anomalies are detected in the western Pacific related to the SAT on the Tibetan Plateau. The SAT on the Tibetan Plateau tends to be warm (cold) when there are positive (negative) SST anomalies in the western Pacific. This positive relationship does not decline even when the linear trend is removed, which is quite different to the variation of SAT in northwestern China. The corresponding correlation coefficient between SAT in the Tibetan Plateau and SST in the western Pacific (10°S–10°N, 110°–150°E) is 0.64 (0.62) before (after) detrending. In contrast, the SST in the tropical eastern Pacific has a relative weak impact on the SAT in western China. The correlation coefficient between SAT in the Tibetan Plateau and the Niño3.4 index is

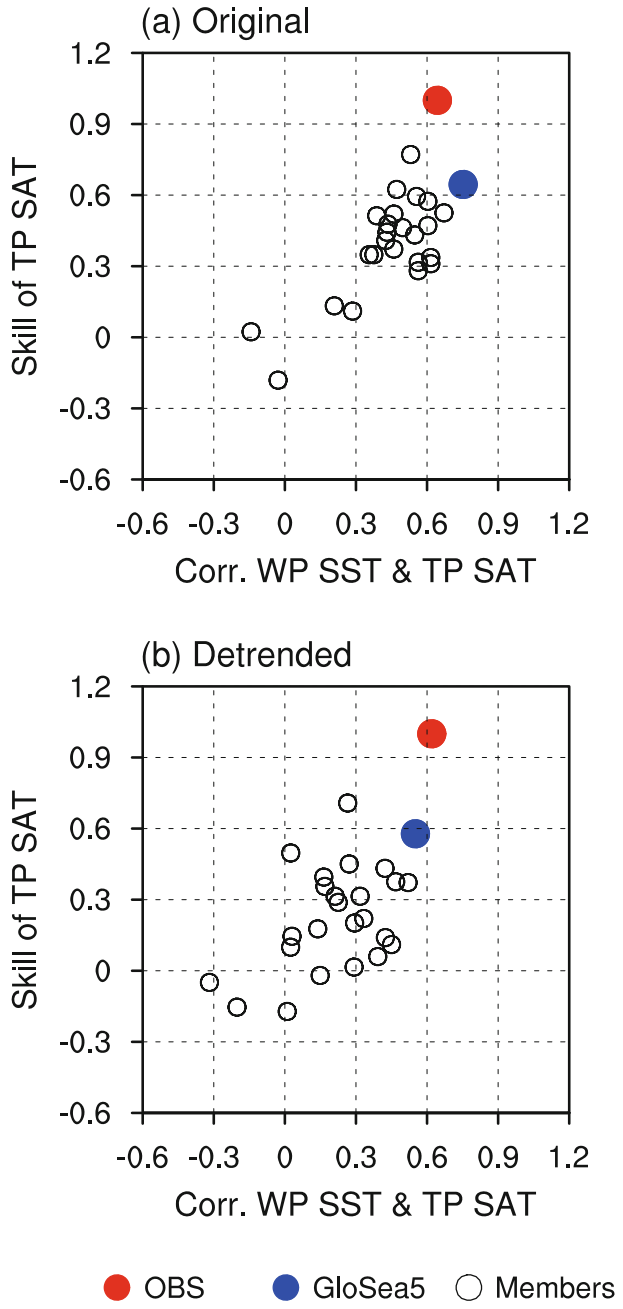

Fig. 9. Scatterplots showing the prediction skill of the (a) original and (b) detrended SAT in the Tibetan Plateau and its relationship with the SST in the western Pacific (box in Fig. 8). The skill is represented by the prediction correlation between the model hindcast and observations, and observations are assumed perfect with a skill of 1. The red solid dot is for the observation; the blue solid dot is for the ensemble mean of GloSea5; and the black hollow dots are for the 24 ensemble members in GloSea5.

−0.39 (−0.33) in observations. GloSea5 demonstrates quite good performance in reproducing this positive relationship, with significantly warm SST in the western Pacific being related to both the original and detrended SAT in the Tibetan Plateau. The significant correlation around the tropical eastern Pacific in the model predictions corresponds to the usage of the ensemble mean result with more predictable signals.

Figure 9 shows the scatterplots for the prediction skill of SAT in the Tibetan Plateau and its relationship with the SST in the western Pacific for observation and prediction from model members. It shows the good performance of the model in capturing the teleconnection of SST in the western Pacific and SAT in the Tibetan Plateau, in associated with the skillful prediction of SAT. The scatter distribution shows a good linear correspondence and suggests that a better description of the teleconnection with the SST in the western Pacific favors a better prediction of SAT in the Tibetan Plateau. The linear correspondence agrees well before and after detrending.

Interannual variation of SST in the western Pacific may modulate the variation of SAT in the Tibetan Plateau and give rise to skillful predictions. Figure 10 illustrates the summer anomalies related to this western Pacific anomalous SST. The SST anomalies in the western Pacific are averaged over the region given by (10°S–10°N, 110°–150°E). Corresponding to an anomalously warm SST in the western Pacific, there is more rainfall around the Maritime Continent and enhanced 500-hPa geopotential height and SAT anomalies around the Indochina Peninsula and the Tibetan Plateau in observations. This kind of pattern is known as a Matsuno–Gill response (Matsuno, 1966; Gill, 1980) forced by the warm SST in the western Pacific. Anomalous condensational heating associated with the increased precipitation around the Maritime Continent, caused by the warming in the western Pacific, tends to excite a warm tropospheric Kelvin wave to the east and an anomalous increase of the 500-hPa geopotential height to the northwest. The surface air around the Tibetan Plateau can thus be warmed by subsidence induced by the increased surrounding geopotential height. In the seasonal predictions, the regression of model members is performed on all the ensemble members in GloSea5, to verify the above process in observation with sufficient sample size. In the model predictions, a related similar response to the warm SST anomalies in the western Pacific occurs, consistent with the above process operating in the model as in observations, and thus effectively giving rise to the high levels of skill in SAT in the Tibetan Plateau.

Moreover, to identify the extent to which the skill of SAT in the Tibetan Plateau can be explained by the western Pacific SST, a cross-validated reforecast is performed using the western Pacific SST as the only predictor. The cross-validated reforecast is built by a statistical linear regression method, leaving one target year out for prediction. After calculation, the cross-validated reforecast result achieves a temporal correlation coefficient of 0.58. It is close to the skill of direct model prediction (0.64) and verifies the western Pacific SST as one of the main sources of the high skill of SAT in the Tibetan Plateau.

5. Summary and discussion

Improved understanding of climate dynamics to enhance regional climate predictions is one of the key research topics

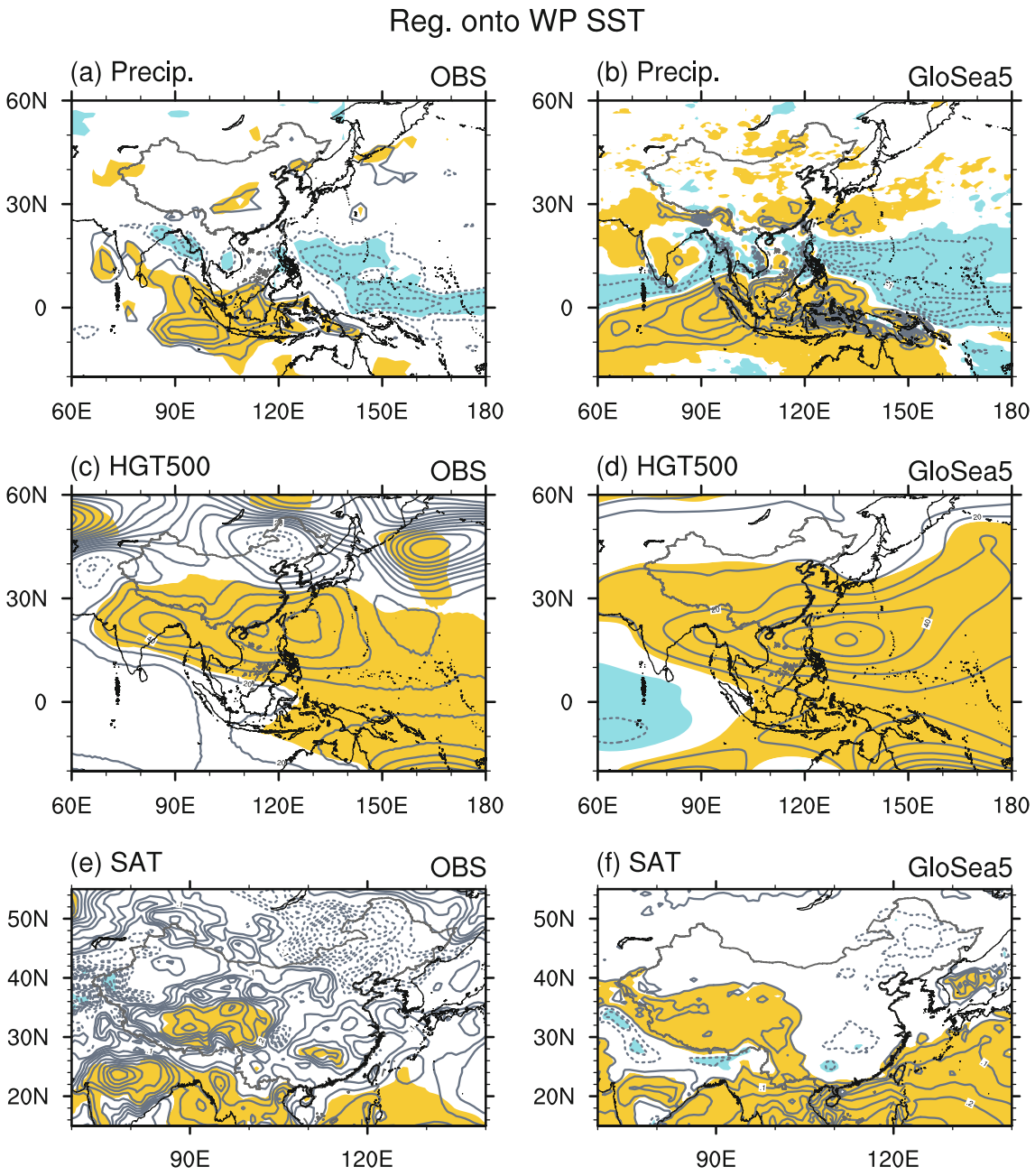

Fig. 10. Regression of (a, b) precipitation, (c, d) 500-hPa geopotential height, and (e, f) SAT anomalies onto the normalized SST anomalies in the western Pacific (box in Fig. 8) for (a, c, e) observations and (b, d, f) the seasonal predictions of all ensemble members in GloSea5. The anomalies are detrended before regression. Shading indicates regions where anomalies exceed the 5% significance level. The contour intervals are 0.5 mm d^{-1}, 10 m, and 0.05°C for the three variables, respectively.

in the Climate Science for Service Partnership China (CSSP China) programme, and is crucial to underpin the development of climate services. In this study, we assess the prediction skill of summer SAT in western China and analyze the dynamical processes that contribute to that predictability, using the GloSea5 forecast system with a 20-year reforecast from 1992 to 2011. We find that the summer variation of SAT is quite skillfully predicted by the forecast system, with considerable temporal correlation coefficients in most regions of western China. The correlation between the model output and observation reaches 0.76 for the SAT averaged over northwestern China, and 0.64 for the Tibetan Plateau.

For the sources of predictability, two important signals are detected: the linear trend and interannual variation of SST in the western Pacific. The SST trend in the tropical Pacific during these 20 years relates closely to the warming trend of SAT in northwestern China. The prediction skill in northwestern China contains a large component from the trend. This implies the importance of reasonable ocean assimilation in skillful prediction of SAT in northwestern China, es-

pecially that over the tropical west Pacific. In contrast, for the Tibetan Plateau, the prediction skill remains high after removing the linear trend. A close teleconnection between the SST variability in the western Pacific and summer SAT around the Tibetan Plateau is revealed. The anomalously warm SST in the western Pacific appears to excite a Matsuno–Gill response with enhanced convection around the Maritime Continent and surface air warming and positive geopotential height over the Tibetan Plateau.

Some midlatitude factors, such as the teleconnection pattern along the Asian upper-tropospheric westerly jet (Hong and Lu, 2016; Lin and Lu, 2016; Lin et al., 2017), which are modulated by atmospheric internal variation and are thus unpredictable (Kosaka et al., 2012), can also affect SAT in western China. This internal "noise" factor may limit the prediction of SAT in western China. The prediction sources identified in this study further confirm that the prediction skill of the current coupled model relies largely on tropical air–sea interactions.

The skillful prediction achieved here suggests a positive outlook for future climate services for disaster mitigation and economic planning. The results presented here also have relevance beyond China: The contribution of interannual SST variation in the western Pacific also helps explain the prediction skill of SAT around the Indochina Peninsula, where skillful predictions with significant impact from the western Pacific SST are also detected (Figs. 2, 4 and 9).

Acknowledgements. This work was supported by the National Key R&D Program of China (Grant No. 2016YFA0600603) and the National Natural Science Foundation of China (Grant Nos. U1502233, 41320104007 and 41775083). This work and its contributors were also supported by the UK–China Research & Innovation Partnership Fund through the Met Office Climate Science for Service Partnership (CSSP) China as part of the Newton Fund.

REFERENCES

Adler, R. F., and Coauthors, 2003: The Version-2 Global Precipitation Climatology Project (GPCP) monthly precipitation analysis (1979–Present). *Journal of Hydrometeorology*, **4**, 1147–1167, https://doi.org/10.1175/1525-7541(2003)004<1147:TVGPCP>2.0.CO;2.

Best, M. J., and Coauthors, 2011: The joint UK land environment simulator (JULES), model description–part 1: Energy and water fluxes. *Geoscientific model Development*, **4**, 677–699, https://doi.org/10.5194/gmd-4-677-2011.

Bett, P. E., and Coauthors, 2017: Skill and reliability of seasonal forecasts for the Chinese energy sector. *Journal of Applied Meteorology and Climatology*, **56**, 3099–3114, https://doi.org/10.1175/jamc-d-17-0070.1.

Bett, P. E., and Coauthors, 2018: Seasonal forecasts of the summer 2016 Yangtze River basin rainfall. *Atmospheric and Oceanic Physics*, https://doi.org/10.1007/s00376-018-7210-y.

Camp, J., M. Roberts, C. MacLachlan, E. Wallace, L. Hermanson, A. Brookshaw, A. Arribas, and A. A. Scaife, 2015: Seasonal forecasting of tropical storms using the Met Office GloSea5 seasonal forecast system. *Quart. J. Roy. Meteor. Soc.*, **141**, 2206–2219, https://doi.org/10.1002/qj.2516.

Chen, J. M., P. Zhao, H. L. Liu, and X. Y. Guo, 2009: Modeling impacts of vegetation in western China on the summer climate of northwestern China. *Adv. Atmos. Sci.*, **26**, 803–812, https://doi.org/10.1007/s00376-009-9018-2.

Clark, R. T., P. E. Bett, H. E. Thornton, and A. A. Scaife, 2017: Skilful seasonal predictions for the European energy industry. *Environmental Research Letters*, **12**, 024002, https://doi.org/10.1088/1748-9326/aa57ab.

Dee, D. P., and Coauthors, 2011: The ERA-Interim reanalysis: Configuration and performance of the data assimilation system. *Quart. J. Roy. Meteor. Soc.*, **137**, 553–597, https://doi.org/10.1002/qj.828.

Ding, H., R. J. Greatbatch, M. Latif, W. Park, and R. Gerdes, 2013: Hindcast of the 1976/77 and 1998/99 climate shifts in the Pacific. *J. Climate*, **26**, 7650–7661, https://doi.org/10.1175/jcli-d-12-00626.1.

Ding, Q. H., and B. Wang, 2005: Circumglobal teleconnection in the Northern Hemisphere summer. *J. Climate*, **18**, 3483–3505, https://doi.org/10.1175/jcli3473.1.

Eade, R., D. Smith, A. Scaife, E. Wallace, N. Dunstone, L. Hermanson, and N. Robinson, 2014: Do seasonal-to-decadal climate predictions underestimate the predictability of the real world? *Geophys. Res. Lett.*, **41**, 5620–5628, https://doi.org/10.1002/2014GL061146.

Gamo, M., 1996: Thickness of the dry convection and large-scale subsidence above deserts. *Bound.-Layer Meteor.*, **79**, 265–278, https://doi.org/10.1007/bf00119441.

Gill, A. E., 1980: Some simple solutions for heat-induced tropical circulation. *Quart. J. Roy. Meteor. Soc.*, **106**, 447–462, https://doi.org/10.1002/qj.49710644905.

Hong, X. W., and R. Lu, 2016: The meridional displacement of the summer Asian jet, Silk Road Pattern, and tropical SST anomalies. *J. Climate*, **29**, 3753–3766, https://doi.org/10.1175/jcli-d-15-0541.1.

Huang, B., and Coauthors, 2015: Extended reconstructed sea surface temperature version 4 (ERSST. v4). Part I: Upgrades and intercomparisons. *J. Climate*, **28**, 911–930, https://doi.org/10.1175/jcli-d-14-00006.1.

Huang, G., X. Qu, and K. Hu, 2011: The impact of the tropical Indian Ocean on South Asian high in boreal summer. *Adv. Atmos. Sci.*, **28**, 421–432, https://doi.org/10.1007/s00376-010-9224-y.

Inoue, T., and J. Matsumoto, 2004: A Comparison of summer sea level pressure over East Eurasia between NCEP-NCAR reanalysis and ERA-40 for the period 1960–99. *J. Meteor. Soc. Japan.*, **82**, 951–958, https://doi.org/10.2151/jmsj.2004.951.

Kosaka, Y., and S.-P. Xie, 2016: The tropical Pacific as a key pacemaker of the variable rates of global warming. *Nature Geoscience*, **9**, 669–674, https://doi.org/10.1038/ngeo2770.

Kosaka, Y., J. S. Chowdary, S.-P. Xie, Y.-M. Min, and J.-Y. Lee, 2012: Limitations of seasonal predictability for summer climate over East Asia and the Northwestern Pacific. *J. Climate*, **25**, 7574–7589, https://doi.org/10.1175/JCLI-D-12-00009.1.

Kumar, A., 2009: Finite samples and uncertainty estimates for skill measures for seasonal prediction. *Mon. Wea. Rev.*, **137**, 2622–2631, https://doi.org/10.1175/2009MWR2814.1.

Kumar, A., M. Y. Chen, and W. Wang, 2013: Understanding prediction skill of seasonal mean precipitation over the tropics. *J. Climate*, **26**, 5674–5681, https://doi.org/10.1175/JCLI-D-12-00731.1.

Li, C. F., and Coauthors, 2016: Skillful seasonal prediction

of Yangtze river valley summer rainfall. *Environmental Research Letters*, **11**, 094002. https://doi.org/10.1088/1748-9326/11/9/094002.

Li, C. F., R. Y. Lu, and B. W. Dong, 2012: Predictability of the western North Pacific summer climate demonstrated by the coupled models of ENSEMBLES. *Climate Dyn*., **39**, 329–346, https://doi.org/10.1007/s00382-011-1274-z.

Li, C. F., R. Y. Lu, and G. H. Chen, 2017: Promising prediction of the monsoon trough and its implication for tropical cyclone activity over the western North Pacific. *Environmental Research Letters*, **12**, 074027, https://doi.org/10.1088/1748-9326/aa71bd.

Lin, Z. D., and R. Y. Lu, 2016: Impact of summer rainfall over southern-central Europe on circumglobal teleconnection. *Atmospheric Science Letters*, **17**, 258–262, https://doi.org/10.1002/asl.652.

Lin, Z. D., F. Liu, B. Wang, R. Y. Lu, and X. Qu, 2017: Southern European rainfall reshapes the early-summer circumglobal teleconnection after the late 1970s. *Climate Dyn*., **48**, 3855–3868, https://doi.org/10.1007/s00382-016-3306-1.

Lu, B., A. A. Scaife, N. Dunstone, D. Smith, H.-L. Ren, Y. Liu, and R. Eade, 2017: Skillful seasonal predictions of winter precipitation over southern China. *Environmental Research Letters*, **12**, 074021, https://doi.org/10.1088/1748-9326/aa739a.

Ma, F., X. Yuan, and A. Z. Ye, 2015: Seasonal drought predictability and forecast skill over China. *J. Geophys. Res*., **120**, 8264–8275, https://doi.org/10.1002/2015JD023185.

MacLachlan, C., and Coauthors, 2015: Global Seasonal forecast system version 5 (GloSea5): A high-resolution seasonal forecast system. *Quart. J. Roy. Meteor. Soc*., **141**, 1072–1084, https://doi.org/10.1002/qj.2396.

Matsuno, T., 1966: Quasi-geostrophic motions in the equatorial area. *J. Meteor. Soc. Japan*., **44**, 25–43, https://doi.org/10.2151/jmsj1965.44.1_25.

Megann, A., D. Storkey, Y. Aksenov, S. Alderson, D. Calvert, T. Graham, P. Hyder, J. Siddorn, and B. Sinha, 2014: GO5.0: The joint NERC–Met Office NEMO global ocean model for use in coupled and forced applications. *Geoscientific Model Development*, **7**, 1069–1092, https://doi.org/10.5194/gmd-7-1069-2014.

Monerie, P.-A., J. Robson, B. Dong, and N. Dunstone, 2017: A role of the Atlantic Ocean in predicting summer surface air temperature over North East Asia? *Climate Dyn*., https://doi.org/10.1007/s00382-017-3935-z.

Palin, E. J., A. A. Scaife, E. Wallace, E. C. D. Pope, A. Arribas, and A. Brookshaw, 2016: Skillful seasonal forecasts of winter disruption to the U.K. transport system. *Journal of Applied Meteorology and Climatology*, **55**, 325–344, https://doi.org/10.1175/jamc-d-15-0102.1.

Qian, Y. F., N. F. Zhou, and Y. Bi, 2004: Analyses of the impacts of upper-level temperature and height anomalies on surface air temperature and precipitation in China. *Plateau Meteorology*, **23**, 417–428, https://doi.org/10.3321/j.issn:1000-0534.2004.04.001. (in Chinese)

Qin, D. H., S. Y. Liu, and P. J. Li, 2006: Snow cover distribution, variability, and response to climate change in western China. *J. Climate*, **19**, 1820–1833, https://doi.org/10.1175/jcli3694.1.

Rae, J. G. L., H. T. Hewitt, A. B. Keen, J. K. Ridley, A. E. West, C. M. Harris, E. C. Hunke, and D. N. Walters, 2015: Development of the global sea ice 6.0 CICE configuration for the Met Office Global Coupled model. *Geoscientific Model Development*, **8**, 2221–2230, https://doi.org/10.5194/gmd-8-2221-2015.

Scaife, A. A., and Coauthors, 2014: Skillful long-range prediction of European and North American winters. *Geophys. Res. Lett*., **41**, 2514–2519, https://doi.org/10.1002/2014GL059637.

Scaife, A. A., and Coauthors, 2017: Tropical rainfall, Rossby waves and regional winter climate predictions. *Quart. J. Roy. Meteor. Soc*., **143**, 1–11, https://doi.org/10.1002/qj.2910.

Smith, D. M., and Coauthors, 2016: Role of volcanic and anthropogenic aerosols in the recent global surface warming slowdown. *Nature Climate Change*, **6**, 936–941, https://doi.org/10.1038/nclimate3058.

Svensson, C., and Coauthors, 2015: Long-range forecasts of UK winter hydrology. *Environmental Research Letters*, **10**, 064006, https://doi.org/10.1088/1748-9326/10/6/064006.

Wang, B., 2008: Thrusts and prospects on understanding and predicting Asian monsoon climate. *Acta Meteorologica Sinica*, **22**, 383–403.

Wang, B., and Coauthors, 2009: Advance and prospectus of seasonal prediction: Assessment of the APCC/CliPAS 14-model ensemble retrospective seasonal prediction (1980-2004). *Climate Dyn*., **33**, 93–117, https://doi.org/10.1007/s00382-008-0460-0.

Wei, K., and W. Chen, 2009: Climatology and trends of high temperature extremes across China in summer. *Atmospheric and Oceanic Science Letters*, **2**, 153–158, https://doi.org/10.1080/16742834.2009.11446795.

Williams, K. D., and Coauthors, 2015: The met office global coupled model 2.0 (GC2) configuration. *Geoscientific Model Development*, **8**, 1509–1524, https://doi.org/10.5194/gmd-8-1509-2015.

Wu, G. X., and Y. M. Liu, 2003: Summertime quadruplet heating pattern in the subtropics and the associated atmospheric circulation. *Geophys. Res. Lett*., **30**, 1201, https://doi.org/10.1029/2002GL016209.

Wu, R., J. L. Kinter III, and B. P. Kirtman, 2005: Discrepancy of interdecadal changes in the Asian region among the NCEP–NCAR reanalysis, objective analyses, and observations. *J. Climate*, **18**, 3048–3067, https://doi.org/10.1175/jcli3465.1.

Yan, L., P. X. Wang, Y. Q. Yu, L. J. Li, and B. Wang, 2010: Potential predictability of sea surface temperature in a coupled ocean-atmosphere GCM. *Adv. Atmos. Sci*., **27**, 921–936, https://doi.org/10.1007/s00376-009-9062-y.

Zhou, L.-T., and R.-H. Huang, 2010: Interdecadal variability of summer rainfall in Northwest China and its possible causes. *International Journal of Climatology*, **30**, 549–557, https://doi.org/10.1002/joc.1923.

Zhou, L. T., and R. H. Huang, 2003: Research on the characteristics of interdecadal variability of summer climate in China and its possible cause. *Climatic and Environmental Research*, **8**, 274–190, https://doi.org/10.3969/j.issn.1006-9585.2003.03.003. (in Chinese)